



Ordering phenomena and demixing in the quasiternary system $\text{Ga}_2\text{Te}_3/\text{Hg}_3\text{Te}_3/\text{In}_2\text{Te}_3$

Harald von Wensierski, Helmut Bolwin, Astrid Zeppenfeld, Volkmar Leute*

Institut für Physikalische Chemie der Universität Münster Schlossplatz 4, D-48149 Münster, Germany

Received 6 September 1996

Abstract

The phase diagram of the quasiternary system

$\text{Ga}_2\text{Te}_3/\text{Hg}_3\text{Te}_3/\text{In}_2\text{Te}_3$

for the temperature range $650 < T/K < 900$ was investigated by X-ray diffraction, by DTA measurements and by electron microprobe analysis. It is shown that ordered structures are formed at special concentrations of structural vacancies. Depending on temperature and concentration, continuous order–disorder transitions could be detected. Besides structural miscibility gaps and a three-phase region, there occurs also a miscibility gap within an ordered region.

Keywords: Ordered phases; Phase diagrams; Phase transitions; Solid solutions; Structural vacancies; Thermodynamics

1. Introduction

The three binary components HgTe, Ga_2Te_3 and In_2Te_3 all crystallize in the zincblende lattice, but because of the 2:3 stoichiometry of the III/VI-components In_2Te_3 and Ga_2Te_3 only 2/3 of the sites in the cationic sublattice of the pure III/VI-components are occupied. Thus, by alloying III/VI-components to II/VI-components, vacancies are introduced into the cationic sublattice of the alloy in a concentration, which is always half that of the trivalent species In and Ga. The unoccupied cationic sites in the zincblende lattice are called structural vacancies, \underline{V} .

Solid solutions, formed from the 3 components HgTe, Ga_2Te_3 and In_2Te_3 , can be described by the expression $(\text{Hg}_{3k_2}, \text{Ga}_{2k_1}, \text{In}_{2(1-k_1-k_2)}, \underline{V}_{4(1-k_1-k_2)})\text{Te}_3$, where k_1 and k_2 are the mole fractions respectively of Ga_2Te_3 and Hg_3Te_3 . The mole fraction of In_2Te_3 is given by $(1-k_1-k_2)$. The equivalent description $(\text{Hg}_{3k_2}, (\text{Ga}, \text{In}_{(1-k_1)})_{2(1-k_2)}, \underline{V}_{4(1-k_2)})\text{Te}_3$ uses the molar ratio $y = n_{\text{Ga}}/(n_{\text{Ga}} + n_{\text{In}})$ instead of the mole fraction k_1 . In the following, the specification of the structural vacancies in the formulas will be omitted.

As shown in preceding papers [1,2], the structural vacancies give rise to ordering processes at special compositions, for example at $k_2 = 0$, $k_2 = 1/4$ and $k_2 = 5/8$. We

will investigate the existence region of the ordered phases and of the disordered solid solutions for dependence on temperature and on composition.

2. Experiments

2.1. Synthesis of binary compounds

The binary compounds HgTe, Ga_2Te_3 and In_2Te_3 were synthesized from the elements (purity of Hg, Ga and In, 99.999%) in evacuated quartz ampoules. Tellurium (purity 99.999%) was previously purified by distillation. The compounds were annealed above their melting point for 15 h and subsequently crystals were grown from the melt by the Bridgman method.

The In_2Te_3 crystals grown by this method show the disordered modification with zincblende structure. To obtain the orthorhombic ordered low temperature modification (space group Imm2) the disordered In_2Te_3 has to be annealed for about 2 weeks at 800 K. The lattice constants of this modification, as measured by the Guinier method, are $a = 435.7$ pm, $b = 1307.2$ pm, $c = 616.2$ pm. These values are in good agreement with those reported by Woolley et al. [3].

*Corresponding author.

2.2. DTA measurements

2.2.1. Experimental details

Because of the high vapor pressure of the Hg chalcogenides the DTA measurements have to be carried out in evacuated sealed quartz ampoules. Both the cooling curves and the heating curves were measured with several constant rates $R=dT/dt$ between 2.5 K/min and 12.5 K/min. The measured onset temperatures were extrapolated to $R=0$ K/min. The melting peaks of Ag, Zn or HgTe ($T_F=945$ K [4]) were taken as reference temperatures.

The enthalpies of fusion for In_2Te_3 and Ga_2Te_3 were calculated by comparison of the areas of their DTA melting peaks with that of HgTe ($\Delta_f H(\text{HgTe})=36.3$ kJ/mol [5])

Substance	T_F/K	$\Delta_f H/\text{kJ/mol}$
Ga_2Te_3	1065 ± 3	48 ± 5
In_2Te_3	940 ± 3	53 ± 5

The temperature of fusion that we measured for Ga_2Te_3 with reference to all three above mentioned standard substances is in good agreement with the value given in the CRC-handbook [6] but deviates by 20 K from the value reported in [7].

2.2.2. Solidus and liquidus curves for the quasibinary section $\text{Hg}_3\text{Te}_3/\text{Ga}_2\text{Te}_3$

Fig. 1 shows the high-temperature part of the phase diagram for the system $\text{Hg}_{3k_2}\text{Ga}_{2-2k_2}\text{V}_{k_2}\text{Te}_3$. Both the HgTe rich alloy with the defect zincblende structure and the tetragonal compound HgGa_2Te_4 with the chalcopyrite structure show a peritectical point. The cubic alloy de-

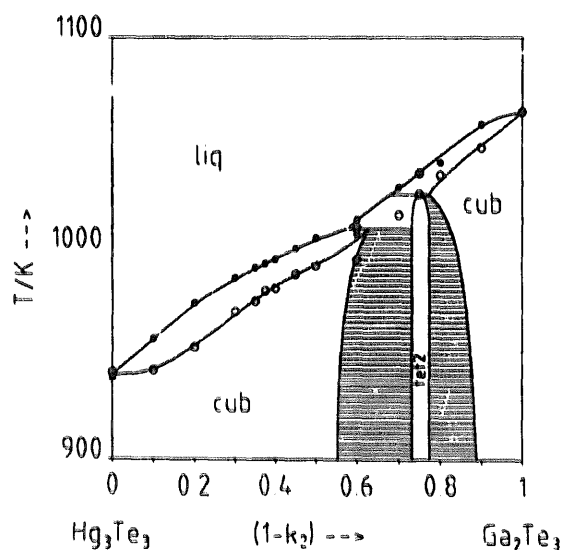


Fig. 1. High temperature part of the phase diagram for the quasibinary section $\text{Hg}_{3k_2}\text{Ga}_{2-2k_2}\text{V}_{k_2}\text{Te}_3$; \circ , DTA heating curves; \square , DTA cooling curves; miscibility gaps between solid phases are hatched.

composes at $k \approx 0.6$. $T_p \approx 1010$ K into the compound HgGa_2Te_4 and the melt and the compound HgGa_2Te_4 at $k=0.75$, $T_p \approx 1025$ K into a Ga_2Te_3 rich cubic solid solution and the melt.

2.2.3. The phase diagram of the quasibinary section $\text{In}_2\text{Te}_3/\text{Ga}_2\text{Te}_3$

Fig. 2 shows the liquidus and solidus curves for the system $\text{In}_{2(1-k_1)}\text{Ga}_{2k_1}\text{V}_{k_1}\text{Te}_3$ as determined from DTA measurements. Moreover, the transition point for the order–disorder transition of pure In_2Te_3 as derived from DTA measurements is shown. The heating curve for the pure orthorhombic In_2Te_3 shows at $T=890$ K a small DTA signal for the transition to the disordered cubic In_2Te_3 as reported in [8]. Corresponding thermal effects for the order–disorder transition in $\text{In}_2\text{Te}_3/\text{Ga}_2\text{Te}_3$ alloys could not be detected.

2.2.4. The order–disorder transition on the quasibinary section at $k_2=5/8$

On the quasibinary section $\text{Hg}_5(\text{Ga}_y\text{In}_{1-y})_2\text{VTe}_3$, the constituents of the cation sublattice can order yielding a tetragonal superstructure of the zincblende lattice ('tet1' structure, space group No. 119, $I\bar{4}m2$). In [1] it was reported that for the compound $\text{Hg}_5\text{Ga}_2\text{Te}_4$ this totally ordered structure exists as a separated superstructure phase with a narrow existence region up to a critical temperature $T_c \approx 770$ K, and that at higher temperatures the same superstructure X-ray reflections still occur, but less sharp and with lower intensity. An equivalent behaviour was observed for $\text{Hg}_5\text{In}_2\text{Te}_4$ [2], where the critical temperature

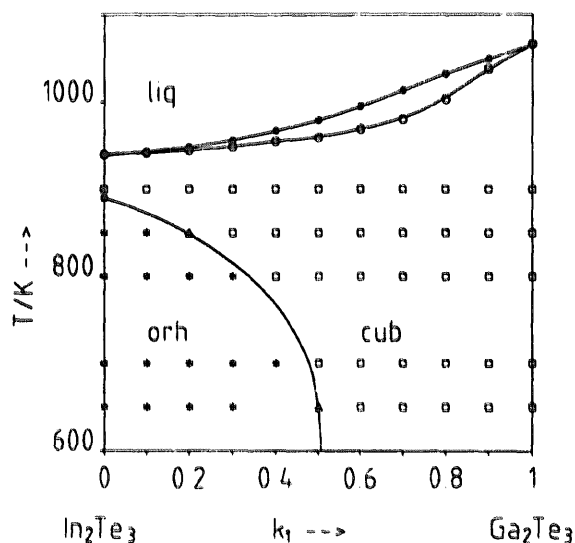


Fig. 2. Phase diagram for the quasibinary section $\text{In}_{2(1-k_1)}\text{Ga}_{2k_1}\text{V}_{k_1}\text{Te}_3$; \circ , DTA heating curves; \square , DTA cooling curves; \blacksquare , DTA value for the orh \rightarrow cub transition. The other symbols correspond to the overall composition of samples investigated by powder X-ray diffraction: $*$, corresponds to Guinier patterns with an orthorhombic set of reflections, \square , with cubic reflections, Δ , with both cubic and orthorhombic reflections.

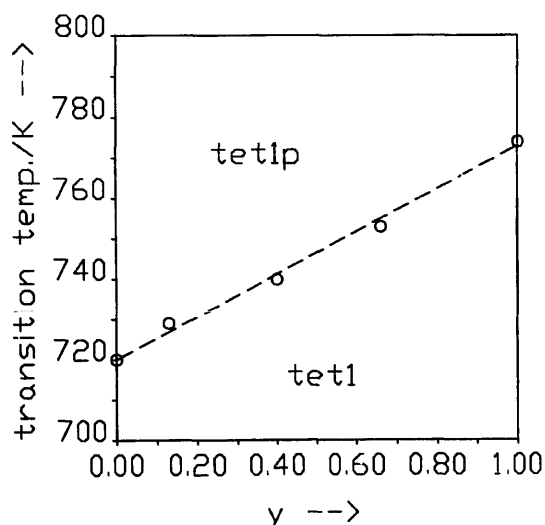


Fig. 3. Critical curve $T_c(y)$, as determined from DTA measurements, for the transition between totally and partially ordered phases at $k(\text{Hg}_1\text{Te}_1) = 5/8$.

is $T_c \approx 720$ K [9,2]. For both substances these critical temperatures could be determined by DTA measurements showing that these transitions are coupled to a thermal effect, as expected for a first order phase transition. DTA measurements on samples of the quasibinary section $\text{Hg}_5(\text{Ga}_y\text{In}_{1-y})_2\text{VTe}_8$ show that the transition temperature changes linearly with y (Fig. 3).

We assume that the low-temperature structure 'tet1' is totally ordered and that above the critical curve the cation lattice is only partially ordered ('tet1p'), in so far as the big Hg^{++} ions are ordered on the b and the four h positions, whereas the vacancies and the smaller trivalent cations are randomly distributed on the a position and the

two f positions. This would also explain the observation that the In/Ga interdiffusion is distinctly faster at temperatures above the critical curve than below [10].

2.3. X-ray diffraction measurements and electron microprobe analysis

2.3.1. General methods

To determine the structures and lattice constants of equilibrium phases in the system $(\text{Hg}_{3k_2}\text{Ga}_{2k_1}\text{In}_{2(1-k_1-k_2)}\text{V}_{(1-k_2)})\text{Te}_3$, a set of powder mixtures of different molar ratios of the binary components were prepared. All samples were annealed in evacuated sealed quartz ampoules until thermodynamic equilibrium was attained. The free volume in these ampoules was filled with a quartz rod to prevent any separation of the mixtures by sublimation. Annealing times ranged between 2 and 4 months, annealing temperatures between 900 K and 650 K. To preserve the high temperature equilibrium composition, the ampoules were quenched in ice-water.

Guinier X-ray measurements on these samples were used to determine the phase diagram. Homogeneous one-phase samples show patterns of reflections corresponding to one of the X-ray patterns plotted in Fig. 4. The structures belonging to these patterns are all well known [3,1,2] with the exception of the so-called domain structure (d) that was also mentioned in [1]. The first two patterns in Fig. 4 correspond to that of the zincblende lattice of HgTe (a) and Ga_2Te_3 (b), the third (tet2) to that of the tetragonal chalcopyrite structure at $k_2 = 1/4$ (c). Pattern (e) shows the set of reflections typical for the tetragonal structure (tet1), and pattern (f) that for the orthorhombic structure of In_2Te_3 (orb).

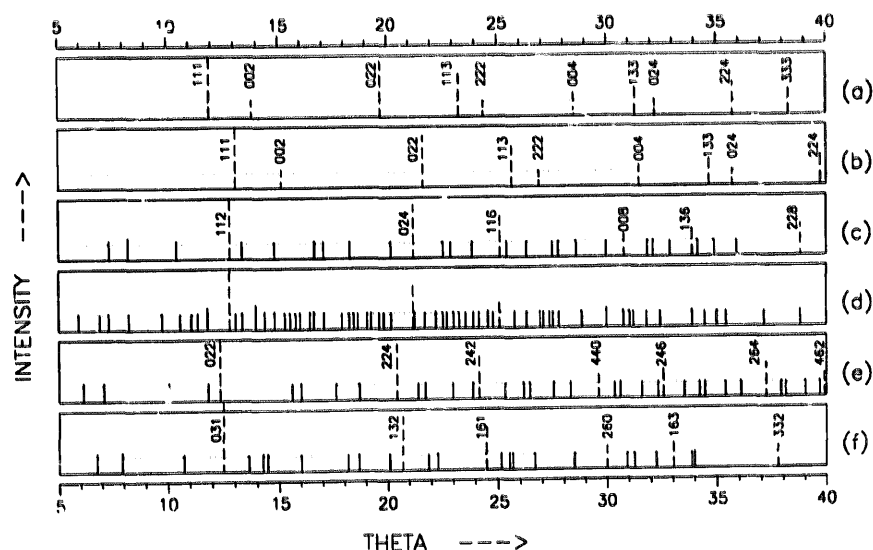


Fig. 4. X-ray patterns of homogeneous solid solutions of type $(\text{Hg}_{3k_2}\text{Ga}_{2k_1}\text{In}_{2(1-k_1-k_2)}\text{V}_{(1-k_2)})\text{Te}_3$, with different structures: (a) HgTe (cub), (b) Ga_2Te_3 (cub), (c) HgGa_2Te_4 (tet2), (d) HgGa_2Te_4 (dom), (e) $\text{Hg}_4\text{Ga}_2\text{Te}_8$ (tet1), (f) In_2Te_3 (orb). Dashed lines: 'zincblende' reflections, solid lines superstructure reflections. The horizontal dotted lines indicate the zero level of X-ray intensity.

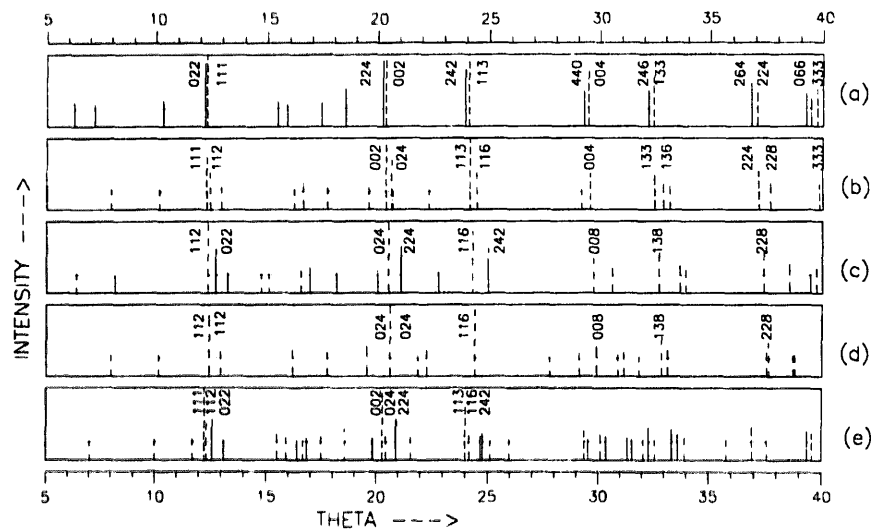


Fig. 5. X-ray patterns of ternary heterogeneous samples for annealing temperatures at which the overall compositions (k_1, k_2) belong to a miscibility gap: (a) $T = 650$ K, (0.15, 0.60), cub/tet1; (b) $T = 900$ K, (0.15, 0.40), cub/tet2; (c) $T = 700$ K, (0.50, 0.40), tet2/tet1; (d) $T = 700$ K, (0.10, 0.20), tet2/tet2; (e) $T = 650$ K, (0.25, 0.53), cub/tet1/tet2; the reflections belonging to different phases were plotted with different line types: - - - cub; — tet1; ··· tet2; - · - tet2 in sample (d) with spinodal demixing. The horizontal dotted lines indicate the zero level of X-ray intensity.

Heterogeneous samples with two (Fig. 5(a)– Fig. 5(d)) or three phases (Fig. 5(e)) in equilibrium show superpositions of patterns belonging either to different structures or, in the case of spinodal miscibility gaps (Fig. 5(d)), belonging to one and the same structure but with different lattice constants.

2.3.2. The cubic lattice constant

All patterns shown in Figs. 4 and 5 show the reflections of the basic 'zincblende' lattice. Thus, as described in [11], we assign a so-called pseudo-cubic lattice constant a^* to all phases showing one of these superstructures of the zincblende lattice. For distorted tetragonal lattices we take a^* as the cube root of the volume of the pseudo-cubic unit cell, i.e. $a^* = (a^2c/2)^{1/3}$ for the distorted chalcopyrite lattice 'tet2', and $a^* = [(a/\sqrt{2})^2c/2]^{1/3}$ for the 'tet1' structure.

In the quasibinary subsystem $\text{In}_{2(1-k_1)}\text{Ga}_{2k_1}\text{VTe}_4$ the composition dependence of the cubic lattice constant (including the pseudo-cubic constant) shows a small positive deviation from the so-called linear Vegard behaviour. The experimental results can best be described by an equation that is cubic in the mole fraction k .

$$a^*(k)/\text{pm} = 616.34 - 21.36k - 8.93k^2 + 4.25k^3 \quad (1)$$

The deviation of the measured values from the values described by this function is less than ± 0.3 pm.

The composition dependence of the cubic lattice constant in the whole quasiternary system $(\text{Hg}_{1-k_1}\text{Ga}_{2k_1}\text{In}_{2(1-k_1-k_2)}\text{V}_{1-k_2})\text{Te}_4$ can be described by a relation being quadratic in k_1 and k_2 :

$$a^*(k_1, k_2)/\text{pm} = A + Bk_1 + Ck_2 + Dk_1^2 + Ek_2^2 + Fk_1k_2 \quad (2)$$

with $A = 616.39$, $B = -22.32$, $C = 21.03$, $D = -3.95$, $E = 10.40$, $F = -3.99$. Fig. 6(a) shows curves for constant values of a^* , projected onto the composition triangle ($k_2 = f(k_1)$). These are the so-called 'isolattice constant lines'.

The difference between measured values and lattice constants calculated according to Eq. (2) never exceeds 0.8 pm for a total of 112 homogeneous samples with compositions widely spread within the regions of solubility (cf. Fig. 7(a),(c),(d),(f)).

2.3.3. Lattice constants of the ordered structures

Fig. 6(b)–(d) show the orthorhombic lattice constants of the ordered alloys of the quasibinary subsystem $(\text{In}_{1-k_1}\text{Ga}_{k_1})_2\text{Te}_4$; all three lattice constants decrease linearly with k . The different symbols correspond to different annealing temperatures as shown for the samples in the 'orh' field of Fig. 2.

Fig. 6(e),(f) describe the composition dependence of the lattice constants a and c for the quasibinary section $\text{Hg}(\text{In}_{1-k_1}\text{Ga}_{k_1})_2\text{Te}_4$ at $k_2 = 1/4$. The lattice constant a of the tetragonal phase 'tet2' changes linearly with y , whereas the constant c shows a bimodal behaviour, i.e. the In–Te bond length is only influenced a little by small contents of Ga in the cation sublattice and vice versa. Thus the c/a ratio decreases from a value of 2.006 at $y = 0$ to ≈ 1.99 near $y = 1$. For pure HgGa_2Te_4 the lattice constants and the c/a ratio depend on temperature as reported in [1], whereas for $y < 1$ a temperature dependence could not be observed.

Fig. 6(g)(h) show the composition dependence of a and c for the quasibinary section $\text{Hg}_5(\text{In}_{1-k_1}\text{Ga}_{k_1})_2\text{Te}_8$ at $k_2 = 5/8$. The lattice constants for the tetragonal unit cell are the same for both the totally ordered structure 'tet1' and the

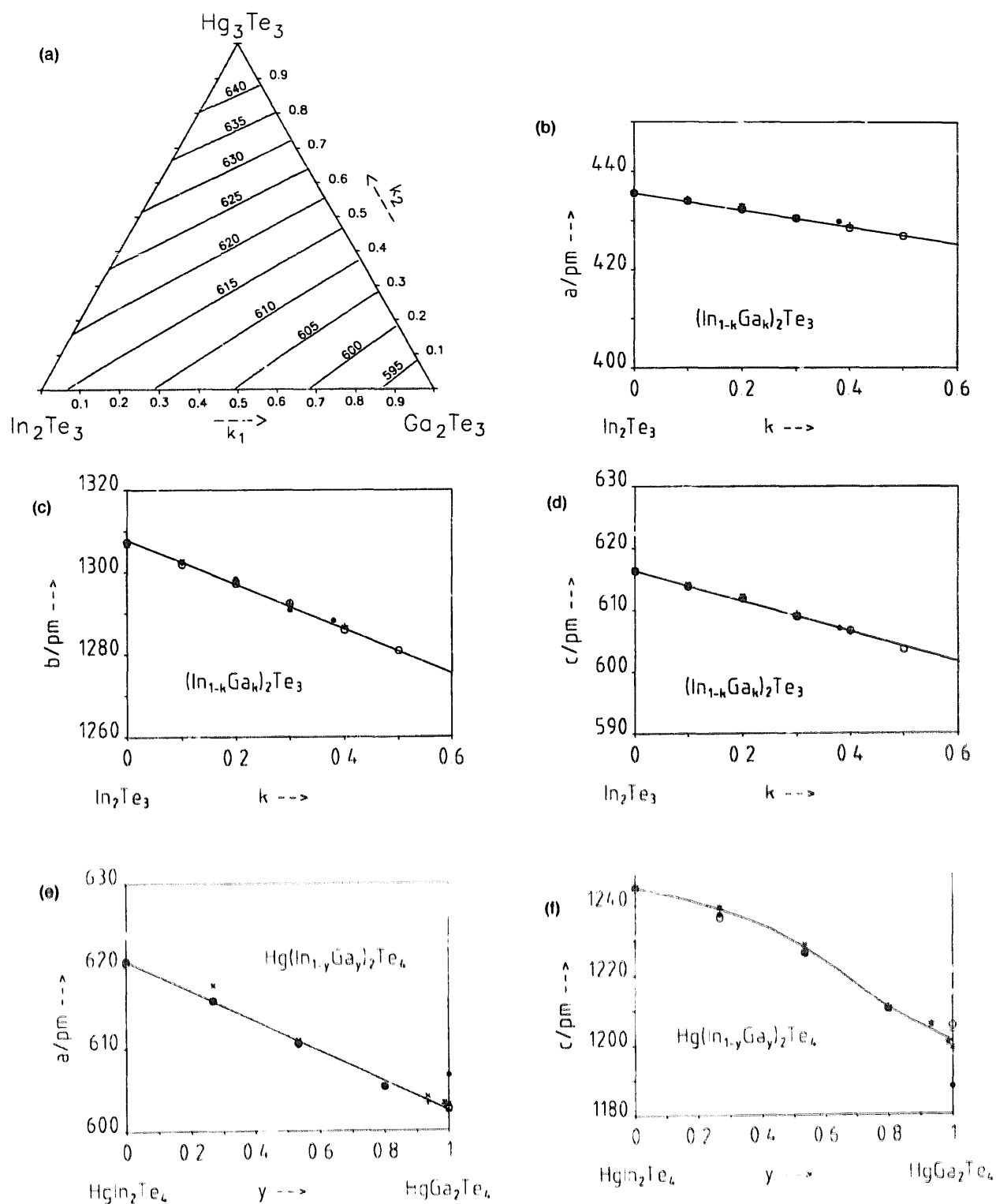


Fig. 6. (a) Isolattice constant lines $k_1 = f(k_2)$. The number on the lines give the lattice constants in units of pm for each of the lines. (b)–(d) Lattice constants a , b and c in dependence on the Ga_2Te_3 mole fraction k for the ordered orthorhombic phase $(\text{In}_{1-k}\text{Ga}_k)_2\text{Te}_3$; the samples were annealed at \circ 650 K, $+$ 700 K, \cdot 800 K, \times 850 K. (e)–(f) Lattice constants a and c of the tetragonal phase 'tet2' in dependence on the composition variable y for the quaternary section $\text{Hg}(\text{In}_{1-y}\text{Ga}_y)_2\text{Te}_4$ at $k_2 = 1/4$; annealing temperatures: \circ 900 K, $+$ 750 K, \times 700 K, \cdot 650 K. (g)–(h) Lattice constants a and c of the tetragonal phase 'tet1' in dependence on the composition variable y for the quaternary section $\text{Hg}_3(\text{In}_{1-y}\text{Ga}_y)_2\text{Te}_4$ at $k_2 = 5/8$; annealing temperatures: \circ 900 K, $+$ 750 K, \times 700 K, \cdot 650 K.

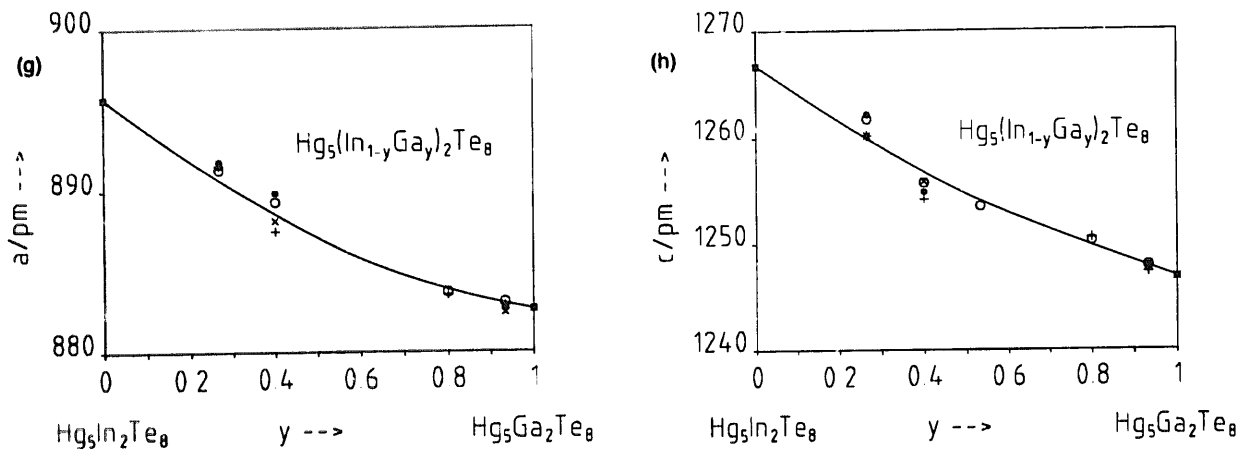


Fig. 6. (continued)

partially ordered structure 'tet1p'. Both constants a and c decrease with increasing y , but faster for In-rich than for Ga-rich alloys.

2.3.4. Tie lines and equilibrium boundaries of miscibility gaps

The directions of the equilibrium tie lines in two-phase regions were determined from Ga, In and Hg X-ray intensity measurements with an electron microprobe at many points on the surface of heterogeneous samples. The composition points calculated from these intensities and the tie lines through the clouds of points are plotted into the composition triangles of Fig. 7(b) and (e). By use of the tie line directions in Fig. 7(b) and (e) and the isolattice constant lines of Fig. 6, the compositions of the equilibrium phases of the heterogeneous samples could be calculated from their lattice constants determined from Guinier films. The principles of this procedure were described in detail in [8].

3. The phase diagram

The quasibinary system $\text{Hg}_{3(1-k)}\text{In}_{2k}\text{V}_k\text{Te}_3$ was already described in [8], the sub-solidus region of the subsystem $\text{Hg}_{3(1-k)}\text{Ga}_{2k}\text{V}_k\text{Te}_3$ in [12].

3.1. The quasibinary subsystem $\text{In}_{2(1-k)}\text{Ga}_{2k}\text{V}_k\text{Te}_3$

3.1.1. Order-disorder transition

The sub-solidus region of this phase diagram is characterized by the transition between the In_2Te_3 -rich orthorhombic ordered phase and the cubic disordered phase (cf. Fig. 2). A miscibility gap between these two phases could not be detected. Two of the whole set of ordered samples, however, did not show all the superstructure reflections but only a few of them. Obviously there is a continuous transition between the ordered and the disordered region. With the exception of pure In_2Te_3 that showed a DTA

signal for the order-disorder transition at $T=890$ K, the phase transition could not be seen in the DTA measurements. Probably the transition changes with increasing Ga_2Te_3 content from a first order transition in pure In_2Te_3 to a second order transition in the solid solutions.

Time dependent measurements ($t/h=3, 6, 12, 60, 2000$) of the phase transition at 750 K from the disordered state to the ordered state for samples with $k_1=0.0, 0.1, 0.2$ and 0.3 (cf. Fig. 2) showed that the ordering process in pure In_2Te_3 is the slowest of all. In this case the orthorhombic reflections could be seen only after the longest annealing time of 2000 h. For $k_1=0.1$ however, these reflections occurred already after 3 h of annealing. With increasing Ga_2Te_3 content, the ordering rate decreases again, but even for $k_1=0.3$ the ordering process is still faster than for $k_1=0$. Most probably, the increase of the transition rate from $k_1=0$ to $k_1=0.1$ is due to the much smaller radius of the dissolved Ga compared to the majority component In [13].

Element	Ionic radius/pm	Covalent radius/pm
Ga	62 (+ + +)	125
In	92 (+ + +)	150
Te	211 (— —)	137

3.1.2. Liquid-solid equilibrium

The liquidus and solidus curves, as measured by DTA (cf. Fig. 2), were used to estimate the thermodynamic interaction parameters for the cubic solid solution. Using the normalized mean molar Gibbs energies for the liquid and the solid phase [14]

$$g^{\text{sol}} = RT[(1-k)\ln(1-k) + k\ln k] + (1-k)k(\alpha^{\text{sol}} + k\beta^{\text{sol}}) \quad (3)$$

$$g^{\text{liq}} = RT[(1-k)\ln(1-k) + k\ln k] + (1-k)k(\alpha^{\text{liq}} + k\beta^{\text{liq}}) + (1-k)\Delta_F H^0(\text{In}_2\text{Te}_3) \times (1 - T/T_F(\text{In}_2\text{Te}_3)) + k\Delta_F H^0(\text{Ga}_2\text{Te}_3)$$

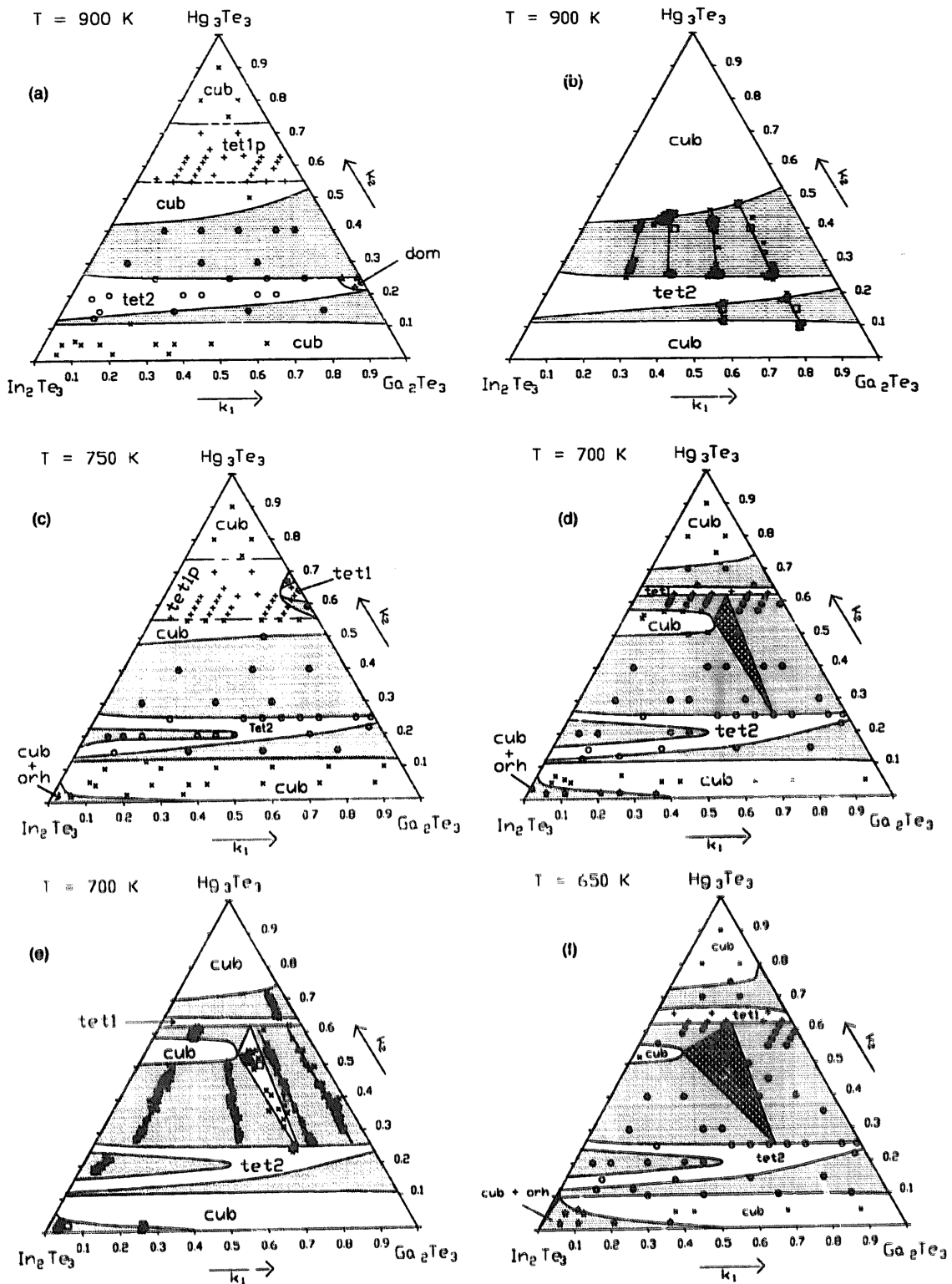


Fig. 7. Isothermal sections of the phase diagram for the quaternary system $(\text{Hg}_{1-x}\text{Ga}_{2x}\text{In}_{2(1-x)}\text{Te}_3)$, as derived from measurements for $T = 900 \text{ K}$ (a),(b), 750 K (c), 700 K (d),(e) and 650 K (f). Dotted areas correspond to two-phase regions, squared areas to three-phase regions. The following symbols correspond to the overall composition of samples that were either homogeneous or heterogeneous after equilibration: \circ , with one cubic set of reflections; $+$, with a tetragonal set of phase (tet1); \times , with a tetragonal set of phase (tet2); \odot , with two tetragonal sets of phase (tet2); \star , with an orthorhombic set of phase (orh). The superposition of several different symbols at one site indicates that the corresponding samples are two- or three-phase samples showing the line sets of the corresponding phases. Data from spot measurements with an electron microprobe (b),(e); \square , overall compositions of the heterogeneous samples; \times , scattered composition values determined at many random dots on the surface of the annealed sample; straight lines through the dot clouds determine tie line directions for the corresponding miscibility gap.

$$\times (1 - T/T_f(\text{Ga}_2\text{Te}_3)) \quad (4)$$

the liquid solid equilibrium is given by $g^{*sol} = g^{*liq}$. With the temperatures and enthalpies of fusion from the DTA measurements we obtained the following interaction parameters:

Phase Φ	$\alpha^\Phi / (\text{kJ/mol})$	$\beta^\Phi / (\text{kJ/mol})$
sol	5.0	-4.0
liq	-1.0	-3.0

These results show that the deviation from ideal mixing behaviour is rather small for In_2Te_3 and becomes even smaller with increasing Ga_2Te_3 mole fraction. Fig. 8 shows the solidus and liquidus lines as calculated with Eq. (3) and (4) together with the DTA data.

3.2. The phase diagram of the quasiternary system

Fig. 7(a)–(f) show several isothermal sections of the phase diagram for the quasiternary system $(\text{Hg}_{3k_1}, \text{Ga}_{2k_1}, \text{In}_{2(1-k_1-k_2)}, \text{V}_{(1-k_2)})\text{Te}_3$ as derived from X-ray diffraction and electron microprobe analysis.

3.2.1. $T = 900 \text{ K}$

At high temperatures (Fig. 7(a)) there are only two miscibility gaps, one between the HgTe-rich solid solution and the phase 'tet2' with the tetragonal chalcopyrite structure, the other between 'tet2' and the cubic $\text{In}_2\text{Te}_3/\text{Ga}_2\text{Te}_3$ -rich alloy region. The phase extension of 'tet2' decreases with increasing mole fraction of k_1 . The so-called domain structure (cf. Fig. 4(d)) that was already observed in the quasibinary subsystem $\text{Hg}_3\text{Te}_3/\text{Ga}_2\text{Te}_3$ [1] extends into the quasiternary region up to an In_2Te_3 mole fraction of about 0.05. A miscibility gap between 'tet2' and this 'dom' phase, showing much more reflec-

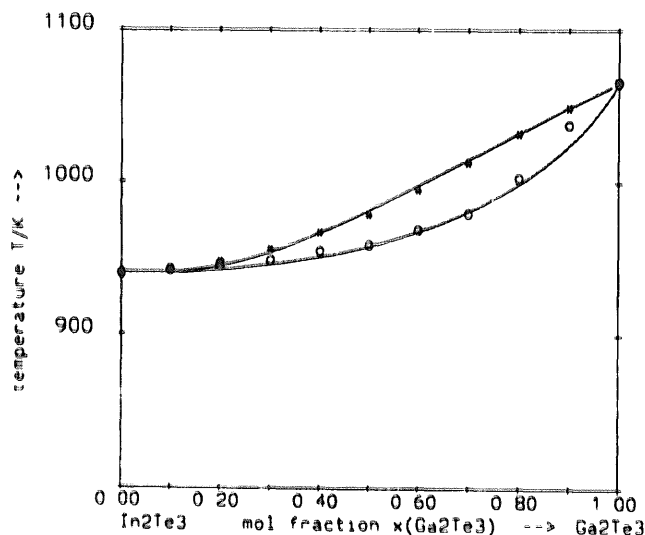


Fig. 8. Solidus and liquidus curves as calculated with Eq. (3) and Eq. (4). \square , DTA liquidus data; \circ , DTA solidus data.

tions than the usual chalcopyrite phase 'tet2', could not be detected.

Within the HgTe-rich alloy region, between $k_2 \approx 0.55$ and 0.7, there is a composition region 'tet1p' yielding additional superstructure reflections of the low temperature phase 'tet1'. But in this case a miscibility gap between this region and the surrounding cubic phase does not exist. For a given ratio γ the reflection patterns show a clearly perceptible dependence on the Hg_3Te_3 mole fraction k_2 . The number and the intensity of the superstructure reflections first increase with increasing k_2 , pass through a maximum at the ideal stoichiometric composition $k_2 = 5/8$, and then decrease again. Obviously, the degree of order of the partially ordered phase 'tet1p' decreases continuously with increasing distance from the stoichiometric composition $k_2 = 5/8$. A similar behaviour was observed in the systems $\text{Hg}_{(3-3k-3l)}\text{Cd}_{3l}\text{Ga}_{2k}\text{Te}_3$ [1] and $\text{Hg}_{(3-3k-3l)}\text{Cd}_{3l}\text{In}_{2k}\text{Te}_3$ [8] near the quasibinary section at $k = 3/8$.

The tie lines plotted in Fig. 7(b) show that the ratio $\gamma = n_{\text{Ga}} / (n_{\text{Ga}} + n_{\text{In}})$ is about the same on both sides of the miscibility gap. Only at low In_2Te_3 mole fractions is the ratio γ distinctly lower in the equilibrium phase being richer in HgTe.

3.2.2. $T = 750 \text{ K}$

With decreasing temperature the phase diagram becomes more complicated:

(a) Near the In_2Te_3 corner of the composition triangle there occurs a narrow quasiternary region for which the X-ray patterns show additional reflections belonging to the ordered orthorhombic phase 'orh'. The cubic reflections of the HgTe-containing solid solution however, could not be separated from the 'zincblende' reflections of the orthorhombic $\text{In}_2\text{Te}_3/\text{Ga}_2\text{Te}_3$ alloy. But a comparison of the measured ratio of the intensities of the 'zincblende' and superstructure reflections with the same ratio calculated for a pure orthorhombic phase, yields intensities of the 'zincblende' reflections being too high for a pure orthorhombic phase. Therefrom, we conclude that there must be an additional disordered cubic phase coexisting with the ordered orthorhombic phase. Thus, a 'cub/orh' miscibility gap with a continuously decreasing width should extend from the In_2Te_3 corner up to the k_1 value corresponding to the value of the transition curve for $T = 750 \text{ K}$ in Fig. 2.

(b) Within the chalcopyrite phase 'tet2' a miscibility gap occurs that extends at $T = 750 \text{ K}$ from the $\text{In}_2\text{Te}_3/\text{Hg}_3\text{Te}_3$ edge ($k_1 = 0$) up to $k_1 \approx 0.4$. As both coexistence borders of this miscibility gap belong to the same phase 'tet2', the instable two-phase region is characterized by a negatively curved part of a single common Gibbs-energy surface. The critical curve for this spinodal miscibility gap starts at ($k_1 = 0, k_2 = 0.8, T_c \approx 860 \text{ K}$ [8]) and extends at constant k_2 with increasing k_1 and decreasing temperature into the 'tet2' phase. Many of the samples belonging to this region

show a pattern with two sets of tetragonal reflections. From the lattice constants calculated from these patterns, the borders of the miscibility gap can be estimated.

(c) On the $\text{Ga}_2\text{Te}_3/\text{Hg}_3\text{Te}_3$ edge of the phase diagram at $k_2 = 5/8$, a new totally ordered phase 'tet1' occurs, being separated from the partially ordered phase 'tet1p' by experimentally realized miscibility gaps. The critical curve for the order–disorder transition between 'tet1' and 'tet1p' is shown in Fig. 3.

$T = 700$ K: With decreasing temperature the ordered phase 'tet1' becomes more and more stable causing an extension of the adjacent miscibility gaps. As the critical line for the order–disorder transition reaches the $\text{In}_2\text{Te}_3/\text{Hg}_3\text{Te}_3$ edge ($y=0$) at 720 K (cf. Fig. 3), the ordered phase 'tet1' extends at 700 K along the whole quasibinary section $\text{Hg}_5(\text{Ga}, \text{In}_{1-y})_2\text{Te}_8$. From [12] we know that for $y=1$ there is an eutectoidic point ('tet1/cub/tet2') at $T \approx 720$ K. At lower temperatures the miscibility gap at $y=1$ reaches from 'tet1' to 'tet2' giving rise to an adjacent three-phase region.

Fig. 7(e) shows the results of the electron microprobe measurements on two- and three-phase samples. The tie lines determined by this method confirm the result derived from the X-ray diffraction measurements. Especially, the microprobe measurements on the In_2Te_3 -rich samples show that there must be a two phase region between the ordered orthorhombic phase 'orh' and the disordered cubic solid solution, as was already derived above from the X-ray intensities.

3.2.3. $T = 650$ K

Compared to 700 K the situation has only changed gradually in so far as the extension of the disordered 'cub' regions has decreased and those of the heterogeneous

regions have increased (Fig. 7(f)). The existence region of the superstructure phase 'tet1' is somewhat broader, whereas that of the chalcopyrite phase 'tet2' remained nearly unchanged.

Acknowledgments

Financial support of this work by the Deutsche Forschungsgemeinschaft and by the Fonds der Chemischen Industrie is acknowledged.

References

- [1] A. Zeppenfeld and V. Leute, *Ber. Bunsenges. Phys. Chem.*, **96** (1992) 1558–1564.
- [2] V. Leute and H.M. Schmidtke, *J. Phys. Chem. Solids*, **49** (1988) 409–420.
- [3] J.C. Woolley, B.R. Pamplin and P.J. Holmes, *J. Less-Common Metals* **1** (1959) 362.
- [4] R.T. Delves and B. Lewis, *J. Phys. Solids*, **24** (1963) 549–556.
- [5] T.D. Levitskaya, A.V. Vanyukov, A.N. Krestivnikov and V.P. Bystrov, *Izv. Akad. Nauk SSSR Neorg. Mater.* **6** (1970) 559.
- [6] R.C. Weast (Ed.), *Handbook of Chemistry and Physics*, 72th. ed., Chemical Rubber Co., 1991–1992.
- [7] R. Blachnik and E. Irlé, *Less-Common Metals*, **113** (1985) L1–L3.
- [8] D. Weitze and V. Leute, *J. Alloys Comp.*, **236** (1996) 229–235.
- [9] B. Ray and P.M. Spencer, *Solid St. Commun.*, **3** (1965) 389.
- [10] H.V. Wensierski and V. Leute, *Solid State Ionics*, (in press).
- [11] D. Weitze, H.M. Schmidtke and V. Leute, *J. Alloys Comp.*, **239** (1996) 117–123.
- [12] V. Leute and A. Zeppenfeld, *Ber. Bunsenges. Phys. Chem.*, **93** (1989) 1227–1230.
- [13] J. Emsley, *The Elements*, Clarendon Press, Oxford, 1989.
- [14] V. Leute and H.J. Köller, *Z. Phys. Chem. Neue Folge*, **149** (1986) 213–227.